Transition Met Chem (2011) 36:283–287
DOI 10.1007/s11243-011-9467-1

Radiosynthesis and characterization of the ^{99m}Tc-fleroxacin complex: a novel *Escherichia coli* infection imaging agent

Syed Qaiser Shah · Muhammad Rafiullah Khan

Received: 8 December 2010 / Accepted: 31 January 2011 / Published online: 26 February 2011

Abstract Radiocomplexation of fleroxacin (FXN) with technetium-99m and its characterization in terms of in vitro stability in saline and serum solutions, in vitro binding with live and heat-killed *Escherichia coli*, and biodistribution in male Wistar rats (MWR) artificially infected with live and heat-killed *E. coli* was studied. The ^{99m}Tc-FXN complex showed a radiochemical purity (RCP) yield of 98.10 ± 0.24% at 30 min using 125 μg of stannous fluoride, 74 MBq of sodium pertechnetate, and 2 mg of FXN. The complex was found to be more than 90% stable up to 4 h after constitution in normal saline. In serum, the emergence of 16.50% undesirable species was observed within 16 h of incubation at 37 °C. The ^{99m}Tc-FXN complex showed saturated in vitro binding with *E. coli* with a maximum value of 65.00% at 90 min. A fivefold increase in uptake of the complex was noted in the infected when compared with the inflamed and normal muscle of the MWR infected with live *E. coli.* The stable radiochemical profile in saline and serum, saturated in vitro binding with *E. coli* and increased uptake in the infected muscle, confirmed the potential of the ^{99m}Tc-FXN complex as an *E. coli* infection imaging agent.

Introduction

Ultrasound (US), computerized tomography (CT), magnetic resonance imaging (MRI), and nuclear medicine imaging (NMI) are the currently available diagnostic techniques for the accurate and timely diagnosis of early-stage infectious foci. NMI is an essential tool for the early detection of infectious processes, as well as discrimination from non-infectious processes, since it can distinguish functional mutilation from structural abnormalities resulting from infection process. The roles of US, CT, and MRI in the early diagnosis of infection are inadequate as the abnormalities arising from structural changes appear late, causing substantial tissue damage [1, 2].

The promising results of the available infection radiotracers, together with our recently reported work [3–15], have motivated us to develop more sensitive and specific radiopharmaceuticals. Fleroxacin [FXN, 6,8-difluoro-1-(2-fluoroethyl)-7-(4-methylpiperazin-1-yl)-4-oxoquinoline-3-carboxylic acid] has recently been established as a novel trifluorinated quinolone antibiotic with promising broad spectrum activity against Gram-positive and Gram-negative bacteria. FXN inhibits gyrase, the enzyme that coils bacterial DNA into its tertiary structure after cell division [16, 17].

In continuation to our ongoing research, we now report the complexation of FXN with technetium-99m and characterization of the ^{99m}Tc-FXN complex in terms of stability in normal saline solution at room temperature, in vitro stability in serum at 37 °C up to 16 h, in vitro binding with *Escherichia coli*, and biodistribution in male Wistar rats (MWR) artificially infected with live and heat-killed *E. coli.*

Experimental

Fleroxacin was obtained from Hangzhou Imaginechem Co., China. Pre-coated TLC plates were obtained from Merck, Germany while all other chemicals and solvents of

S. Q. Shah (✉)
Nuclear Medicine Research Laboratory (NMRL), University of Peshawar, Peshawar, KPK, Pakistan
e-mail: ssqaiser2002@yahoo.com

M. R. Khan
Phytopharmaceutical & Neutraceuticals Research Laboratory (PNRL), University of Peshawar, Peshawar, KPK, Pakistan

analytical grade were from Sigma. RP-HPLC was done with a Shimadzu instrument. A well counter and scalar count rate meter were supplied by Ludlum, USA. A dose calibrator manufactured by Capintech, USA, and a Gamma camera GKS-1000 (GEADE Nuclearmedizine of Germany) were used.

Synthesis of the complex

Stannous fluoride (25 to 250 μg in 25 μg increments) was separately taken in ten nitrogen-filled vials through a sterilized syringe. Thereafter, 18.5–185 MBq in 18.5 MBq increments of sodium pertechnetate were added in chronological order to the vials aseptically. Subsequently, 0.5 to 5.0 mg in 0.5 mg increments of FXN was added to the above preparations and the pH was adjusted to 5.5 with 0.01 N HCl. The vials were incubated at room temperature for 10 min and then filtered through a Millipore filter (pore size 0.22 μm, water flow rate 6.7 mL/min/cm^2, air flow rate 2 L/min/cm^2).

HPLC characterization

The complex was characterized in normal saline in terms of radiochemical purity (RCP) using HPLC as reported earlier [9]. Briefly, 10 μL of freshly synthesized complex was injected into the HPLC system equipped with a UV detector operating at 254 nm and C-18 (4.6 × 150 mm) column (Shimadzu). The sample was eluted with a mobile phase consisting of triethylaminophosphate (A) and methyl alcohol (B) for 15 min with a flow rate of 1 mL/min. The mobile phase for 0–3 min (100%: A), 3–6 min (100–75% A), 6-8 min (75–66% A), 8–10 min (34–100% B), 10–12 min (100% B), and 12–15 min (100% B to 100% A) was employed. The radio-fractions (1 mL/min) received during 1–15 min of elution were measured for radioactivity using a single well counter interface with scalar count rate meter (SWCR).

In vitro stability in serum

In serum, in vitro stability of the complex was studied up to 16 h at 37 °C using the method reported earlier [12]. Briefly, 1.8 mL of the fresh serum was incubated with 0.2 mL of the complex at 37 °C for 16 h. During incubation, aliquots were removed from the mixture after 0, 2, 4, 6, 8, 10, 12, 14, and 16 h and spotted onto TLC (silica gel) strips. The strips were developed using (CH_2Cl_2:CH_3OH (9:1) (v/v) mobile phase. Thereafter, each strip was divided into two parts at ($R_f = 0.5$) and counted for activity in each strip using SWCR.

In vitro binding with *Escherichia coli*

The in vitro binding behavior of the complex with live and heat-killed *E. coli* was studied according to the reported method [18]. Briefly, 0.1 mL of sodium phosphate buffer (Na–PB) was vortexed with 0.2 mL of the complex. Then, 0.8 mL (50% v/v) 0.01 M acetic acid containing 1×10^8 colony-forming units (CFU) of *E. coli* was added to the blend followed by incubation for 1 h at 4 °C at pH 5. Thereafter, the blend was centrifuged at 2000 rpm for 10 min. The supernatant from the test tube was removed, and the bacterial pellets were resuspended in 2 mL Na–PB and processed again at 2000 rpm for 10 min. The supernatant was again removed leaving the bacterial pellets in the test tube, which were counted for percent uptake using SWCR.

Biodistribution in a Wistar model

The in vivo uptake of the complex a range of tissues of MWR artificially infected with live and heat-killed *E. coli* was evaluated at 30, 60, 90, and 120 min. Fourteen healthy MWR (weight 150–170 g) were segregated into two groups (designated A and B). A 0.2-mL injection of sterile turpentine oil was intramuscularly (I.M.) administered to both groups followed by I.M. injection of live *E. coli* (0.2 mL in saline) to the contra lateral thighs of the MWR group A and heat-killed *E. coli* to group B. After 24 h, 0.2 mL of the complex was administered intravenously (i.v.) to both groups. In accordance with the Nuclear Medicine Research Laboratory (NMRL) University of Peshawar rules, both groups were then killed. Thereafter, percentage uptake of the complex in one gram of the blood, liver, spleen, stomach, intestines, kidneys, infected, inflamed, and normal muscles of MWR was calculated using SWCR.

Results and discussion

Radiochemistry and structural formula of the complex

The complex as shown in Fig. 1 was prepared by reducing ^{99m}Tc in pertechnetate with stannous fluoride. The concentration of the reacting species at which the complex showed maximum RCP yield (98.10 ± 0.24% at 30 min) was 125 μg of stannous fluoride, 74 MBq of sodium pertechnetate, and 2 mg of FXN, as shown in Fig. 2. The RCP values of the complex decreased to 90.55 ± 0.22% within 240 min after reconstitution. The RCP yields of the complex at different intervals are given in Fig. 3.

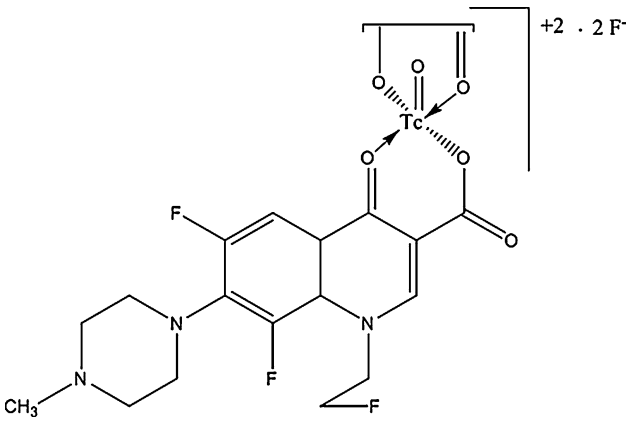

Fig. 1 Structure of the ^{99m}Tc-FXN complex

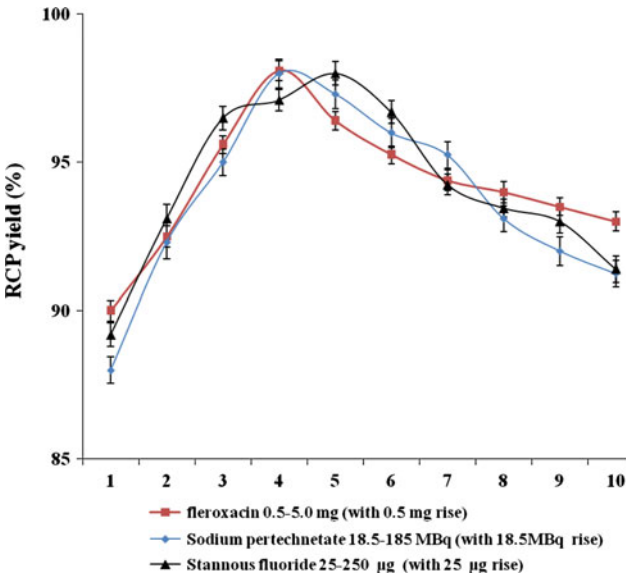

Fig. 2 Effect of FXN, sodium pertechnetate, and stannous fluoride on the radiochemical purity (RCP) yield of the ^{99m}Tc-FXN complex

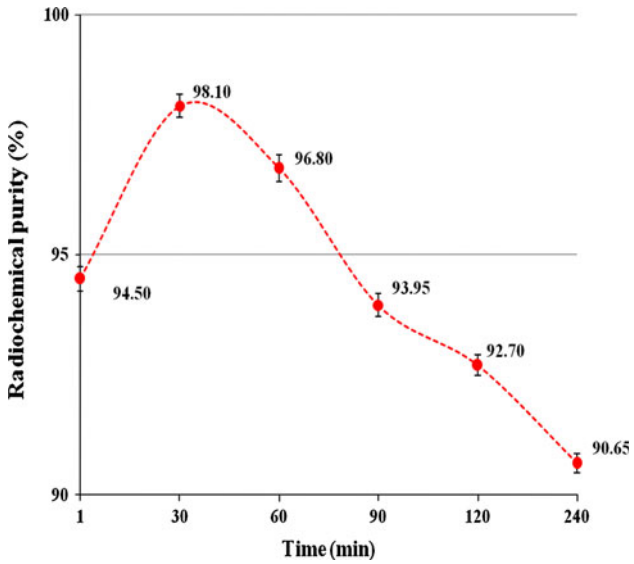

Fig. 3 Radiochemical stability of the ^{99m}Tc-FXN complex in normal saline at different intervals

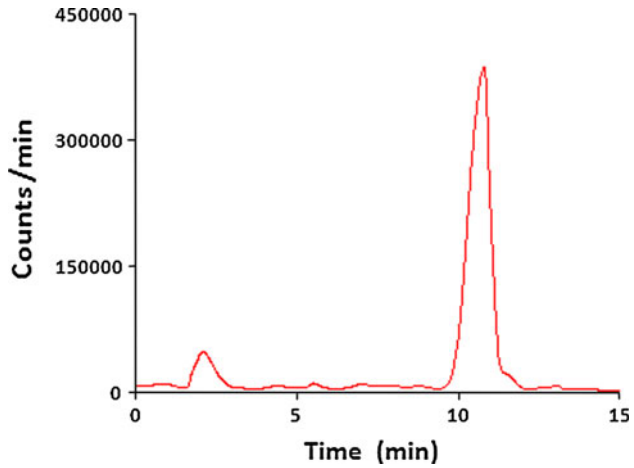

Fig. 4 HPLC radiochromatogram of the 99mTc-FXN complex

The structural features of the Tc=O complexes can be explained on the basis of the reported [19] structure of Tc≡N. Technetium can have a number of oxidation states but the +V state is the most common in Tc≡N and Tc=O complexes, with d^2 configuration. Crystal structural studies have shown that when the atoms involved in coordination are π-donor Lewis bases as in the present case then the square pyramidal structure is highly preferred [20]. Based on the above explanation, this Tc^{v}=O complex (Fig. 1) will have a square pyramidal configuration having ^{99m}Tc to FXN ratio of 1: 2.

Two different peaks with 2.1- and 10.9-min retention times were observed, as shown in Fig. 4. The peak at 2.1 min is assigned to free technetium-99 m and the peak at 10.9 min the ^{99m}Tc-FXN complex. The stability of the complex after 16 h at 37 °C was determined by TLC. The quantity of side product after 16 h was 16.50% as shown in Fig. 5.

Binding to *E. coli* and biodistribution

The in vitro binding behavior of the complex with live and heat-killed *E. coli* at different intervals is given in Table 1. The complex showed maximum binding of 65.00% at 90 min with live *E. coli*. Significantly lower binding was observed with heat-killed *E. coli*.

The in vivo uptakes of the complex in various tissues of MWR artificially infected with live and heat-killed *E. coli*, evaluated at 30, 60, 90, and 120 min are given in Table 2. The level of activity of the complex in 1 gram of blood

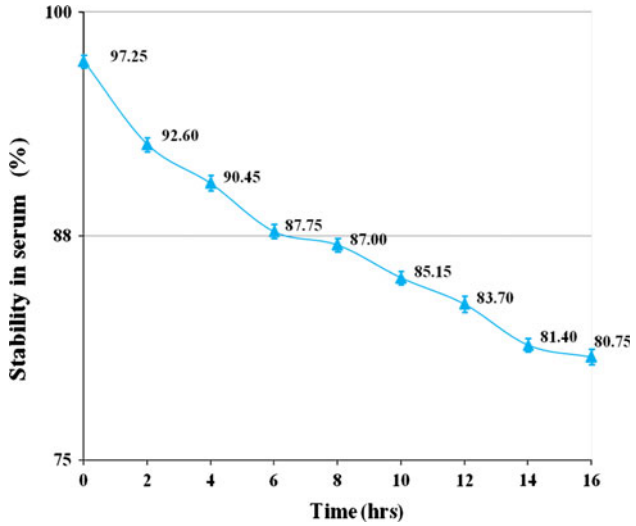

Fig. 5 In vitro stability of the ^{99m}Tc-FXN complex in serum

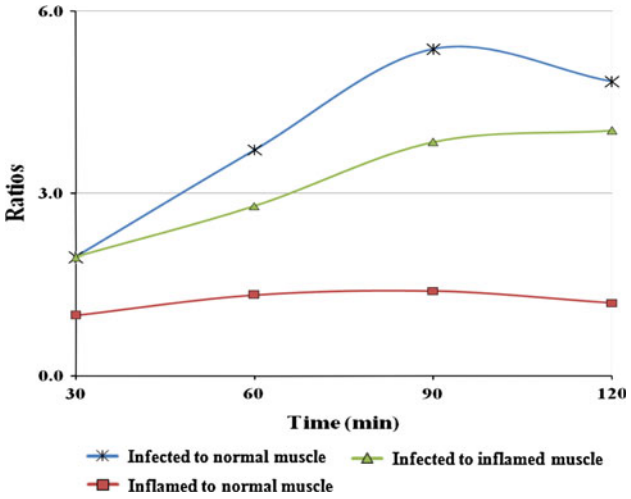

Fig. 6 Infected to normal, inflamed to normal, and infected to inflamed muscles ratios of the ^{99m}Tc-FXN complex

(group A) was initially high but decreased from 20.15 ± 0.26 to 4.20 ± 0.20% within 120 min. Similarly, the level of the complex in liver, spleen, stomach, and intestines decreased within 120 min of I.V. administration. However, for the kidneys, the complex showed increasing uptake, wherein the activity of the complex increased from 9.45 ± 0.24 to 23.25 ± 0.24% within 120 min. Analogous uptakes were seen in the blood, liver, spleen, stomach, intestines, and kidneys of group B MWR. However, significantly different uptakes were observed in the infected, inflamed, and normal muscles of groups A and B. The uptake of the complex observed in the infected muscle of the group A was fivefold higher than the inflamed and normal muscles. However, no significant difference was observed in the uptake of the complex in the infected, inflamed, and normal muscles of group B. The ratio uptakes in groups A and B are shown in Fig. 6. The accumulation of activity in the urinary system and reduction from the circulatory system established the standard course of excretion of the complex.

Table 1 In vitro binding of the live and heat-killed *Escherichia coli* with the ^{99m}Tc-FXN complex

In vitro binding with	Percent in vitro binding with *Escherichia coli* at different intervals (min.)			
	30	60	90	120
Live *E. coli*	29.25 ± 0.45	55.75 ± 0.50	67.25 ± 0.40	60.50 ± 0.55
Heat-killed *E. coli*	14.75 ± 0.70	17.50 ± 0.65	15.25 ± 0.70	12.50 ± 0.75

Table 2 The in vivo percent (%) uptake of the ^{99m}Tc-FXN complex in per gram (g) of the blood, liver, spleen, stomach, intestines, kidneys, infected, inflamed, and normal muscles of the MWR artificially infected with live and heat-killed *E. coli*

Organs/tissues (gm)	Percent in vivo absorption at different intervals (in min)							
	Live *E. coli*				Heat-killed *E. coli*			
	30	60	90	120	30	60	90	120
Infected muscle	5.85 ± 0.22	11.15 ± 0.24	13.45 ± 0.20	12.10 ± 0.26	3.00 ± 0.24	3.50 ± 0.26	3.00 ± 0.26	2.50 ± 0.22
Inflamed muscle	3.00 ± 0.24	4.00 ± 0.20	3.50 ± 0.26	3.00 ± 0.20	3.00 ± 0.22	4.50 ± 0.24	3.50 ± 0.00	3.00 ± 0.26
Normal muscle	3.00 ± 0.22	3.00 ± 0.24	2.50 ± 0.20	2.50 ± 0.24	3.00 ± 0.26	3.00 ± 0.20	2.50 ± 0.24	2.50 ± 0.00
Blood	20.15 ± 0.26	11.20 ± 0.22	9.35 ± 0.24	4.20 ± 0.20	19.80 ± 0.20	11.40 ± 0.00	9.30 ± 0.24	4.25 ± 0.22
Liver	19.00 ± 0.24	11.70 ± 0.22	9.40 ± 0.20	4.90 ± 0.00	19.25 ± 0.22	12.10 ± 0.20	10.00 ± 0.24	5.10 ± 0.26
Spleen	9.30 ± 0.26	7.40 ± 0.20	6.20 ± 0.24	4.30 ± 0.20	9.25 ± 0.22	7.80 ± 0.24	6.60 ± 0.20	4.50 ± 0.24
Kidney	9.45 ± 0.24	17.45 ± 0.22	19.75 ± 0.00	23.25 ± 0.24	10.00 ± 0.22	17.85 ± 0.00	20.40 ± 0.24	23.60 ± 0.20
Stomach & intestines	9.30 ± 0.20	7.25 ± 0.24	6.50 ± 0.22	4.10 ± 0.00	10.00 ± 0.26	7.50 ± 0.20	6.65 ± 0.24	4.25 ± 0.22

Conclusion

Complexation of fleroxacin with technetium-99 m and its biological characterization have been studied in artificially infected male Wistar rats with live and heat-killed *E. coli.* Based on the stable radiochemical profile in saline and serum, saturated in vitro binding with *E. coli* and fivefold uptake in the infected muscle when compared with the inflamed and normal muscles, we propose that this complex is a promising *E. coli* infection imaging agent.

References

1. Gallagher H, Ramsay SC, Barnes J, Maggs J, Cassidy N, Ketheesan N (2006) Neutrophil labeling with [^{99m}Tc]-technetium stannous colloid is complement receptor 3-mediated and increases the neutrophil priming response to lipopolysaccharide. Nucl Med Biol 33:433
2. Stumpe KDM, Dazzi H, Schaffner A, Schulthess GK (2000) Infection imaging using whole-body FDG-PET. Eur J Nucl Med 27:822
3. Chattopadhyay S, Das SS, Chandra S, De K, Mishra M, Sarkar BR, Sinha S, Ganguly S (2010) Synthesis and evaluation of ^{99m}Tc-moxifloxacin, a potential infection specific imaging agent. Appl Radiat Isotopes 68:314
4. Zhang J, Guo H, Zhang S, Lin Y, Wang X (2008) Synthesis and biodistribution of a novel ^{99m}TcN complex of ciprofloxacin dithiocarbamate as a potential agent for infection imaging. Bioorg Med Chem Lett 18:51
5. Oh SJ, Ryu J, Shin JW, Yoon EJ, Ha H, Cheon JH, Lee HK (2002) Synthesis of ^{99m}Tc-ciprofloxacin by different methods and its biodistribution. Appl Radiat Isoptopes 57:193
6. Motaleb MA (2009) Preparation, quality control and stability of ^{99m}Tc-sparafloxacin complex a novel agent for detecting sites of infection. J Label Compd Radiopharm 52:415
7. Qaiser SS, Khan AU, Khan (2010) Synthesis, biodistribution and evaluation of ^{99m}Tc-Sitafloxacin kit : a novel infection imaging agent. J Radioanal Nucl Chem 284:189
8. Shah SQ, Khan AU, Khan MR (2010) Radiosynthesis of ^{99m}Tc-nitrifuratonin a novel radiotracer for in vivo imaging of *Escherichia coli* infection. J Radioanal Nucl Chem. Online published on 19 August 2010
9. Shah SQ, Khan AU, Khan (2010) Radiosynthesis and biodistribution of ^{99m}Tc-rifampicin: a novel radiotracer for in vivo infection imaging. Appl Radiat Isot 68:2255
10. Shah SQ, Khan AU, Khan MR (2010) ^{99m}Tc-Novobiocin: a novel radiotracer for infection imaging. Radiochimica acta (in press)
11. Shah SQ, Khan AU, Khan MR (2010) Radiosynthesis, biodistribution and scintigraphy of the ^{99m}Tc-Teicoplanin complex in artificially infected animal models. J Label Compd Radiopharm (in press)
12. Shah SQ, Khan AU, Khan MR (2010) Radiosynthesis and biological evaluation of ^{99m}TcN-sitafloxacin dithiocarbamate as potential radiotracer for *Staphylococcus aureus* infection J Radioanal Nucl Chem. Online published on 19 September 2010
13. Shah SQ, Khan AU, Khan MR (2010) Radiosynthesis and biodistribution of ^{99m}TcN-Garenoxacin dithiocarbamate complex a potential infection imaging agent. J Radioanal Nucl Chem. (Accepted 06 October 2010) (in press)
14. Shah SQ, Khan AU, Khan MR (2010) Radiosynthesis and biological evolution of ^{99m}Tc(CO)$_3$-sitafloxacin dithiocarbamate complex: a promising *Staphylococcus aureus* infection radiotracer. J Radioanal Nucl Chem. (Accepted 11 October 2010) (in press)
15. Shah SQ, Khan AU, Khan MR (2010) ^{99m}Tc(CO)$_3$-Garenoxacin dithiocarbamate synthesis and biological evolution in rats infected with multiresistant *Staphylococcus aureus* and penicillin-resistant *Streptococci.*. J Radioanal Nucl Chem. (Accepted 18 October 2010) (in press)
16. Kapetanovi V, Milovanovi L, Aleksi M, Ignjatovi L (2000) Voltammetric methods for analytical determination of fleroxacin in Quinodis® tablets. J Pharm Biomed Anal 22:925
17. Djurdjevic P, Jelikic-Stankov M, Laban A (2001) High-performance liquid chromatographic assay of fleroxacin in human serum using fluorescence detection. Talanta 55:631
18. Welling MM, Paulusma-Annema A, Batler HS, Pauwels EKJ, Nibbering PH (2000) Technetium-99m labelled antimicrobial peptides discriminate between bacterial infections and sterile inflammations. Eur J Nucl Med 27:292
19. Boschi A, Duatti A, Uccelli L (2005) Development of technetium-99m and rhenium-188 radiopharmacueticals containing a terminal metal-nitrido multiple bond for diagnosis and therapy. Top Curr Chem 252:85
20. Bandoli G, Dolmella A, Porchia M, Tisato E, Refosco P (2001) Structural overview of technetium compounds (1993–1999. Coord Chem Rev 214:43